

Dijet azimuthal decorrelations at the LHC in the parton Reggeization approach

M. A. Nefedov^{a*}, V. A. Saleev^{a†}, A.V. Shipilova^{a‡}

^a *Samara State University*

Ac. Pavlov 1, 443011 Samara, Russia

Abstract

We study inclusive dijet azimuthal decorrelations in proton-proton collisions at the CERN LHC invoking the hypothesis of parton Reggeization in t -channel exchanges at high energies. In the parton Reggeization approach, the main contribution to the azimuthal angle difference between the two most energetic jets comes from the process of fusion of two Reggeized gluons into a pair of Yang-Mills gluons. We use the high-energy factorization scheme with the Kimber-Martin-Ryskin unintegrated parton distribution functions and the Fadin-Lipatov effective vertices and obtain a good agreement of our calculations with recent measurements by the ATLAS and CMS Collaborations at the CERN LHC.

1 Introduction

The production of large transverse-momentum (p_T) hadron jets at the high-energy colliders is an important source of information about dynamics of parton-parton interactions at small distances and parton distribution functions (PDF), and a good test of perturbative quantum chromodynamics (pQCD) [1]. The measurements of decorrelations in the azimuthal angle between the two most energetic jets, $\Delta\varphi$, as a function of number of produced jets, give the chance to separate directly leading order (LO) and next-to-leading orders (NLO) contributions in the strong coupling constant α_s . Furthermore, a precise understanding of the physics of events with large azimuthal decorrelations is essential for the search of new physical phenomena with dijet signatures by the CMS [2] and ATLAS [3] detectors at the LHC.

The total collision energies at the LHC, $\sqrt{S} = 7$ TeV or 14 TeV, sufficiently exceed the transverse momenta of identified jets ($0.1 < p_T < 1.3$ TeV). The recent theoretical studies of single jet production at high energy show the dominance of the multi-Regge final states in the inclusive production cross sections [4], which means a dominance of partonic subprocesses involving t -channel parton exchanges. These t -channel partons become Reggeized, being off-shell and carrying non-zero transverse momenta. As it has been shown by Lipatov and co-authors, Reggeized gluons and quarks are the appropriate gauge-invariant degrees of freedom of high-energy pQCD.

The parton Reggeization approach (PRA) [5, 6] is based on an effective quantum field theory implemented with the non-Abelian gauge-invariant action which includes fields of Reggeized gluons [7] and Reggeized quarks [8]. Recently, this approach was successfully applied to interpret the p_T -spectra of inclusive production of single jet [4], prompt-photon [9, 10], Drell-Yan lepton pairs [11] and bottom-flavored jets [12, 13] at the Tevatron and LHC.

The single jet production is dominated by the multi-Regge kinematics (MRK), when only a jet with a highest transverse momentum (leading jet) is produced in the central rapidity region,

*e-mail: nefedovma@gmail.com

†e-mail: saleev@samsu.ru

‡e-mail: alexshipilova@samsu.ru

being strongly separated in rapidity from other particles. If the same situation is realized for two or more the most energetic jets, then quasi-multi-Regge kinematics (QMRK) is at work.

In the present work we study azimuthal decorrelations between the two central jets with the largest transverse momenta according to the measurements implemented by the CMS and ATLAS Collaborations [2, 3]. The more extended analysis the reader can find in our work [14].

2 Dijet production in QMRK

In the high-energy Regge limit, when the collision energy is very high but the transverse momenta of produced jets are fixed by the condition $\sqrt{S} \gg p_T \gg \Lambda_{QCD}$, the high-energy (uncollinear) factorization works well instead of collinear parton model. In this case, the Balitsky-Fadin-Kuraev-Lipatov (BFKL) QCD-evolution of unintegrated PDFs [15] can be more adequate approximation than the Dokshitzer-Gribov-Lipatov-Altarelli-Parisi (DGLAP) QCD-evolution of collinear PDFs [16]. It means, that we need to consider the processes with strong ordering in rapidity at the MRK or QMRK conditions. We identify final-state jets and final-state partons, and consider production of two partons in the central region of rapidity, assuming that there are no any other partons with the same rapidity. To the LO in the parton Reggeization approach we have the following partonic subprocesses, which describe production of two central jets in proton-proton collisions: $R+R \rightarrow g+g$ (1), $R+R \rightarrow q+\bar{q}$ (2), $Q+R \rightarrow q+g$ (3), $Q+Q \rightarrow q+q$ (4), $Q+Q' \rightarrow q+q'$ (5), $Q+\bar{Q} \rightarrow q+\bar{q}$ (6), $Q+\bar{Q} \rightarrow q'+\bar{q}'$ (7), $Q+\bar{Q} \rightarrow g+g$ (8), where R is a Reggeized gluon, Q is a Reggeized quark, g is a Yang-Mills gluon, q is an ordinary quark, q and q' denote quarks of different flavors. Working in the center-of-mass (c.m.) frame, we write the four-momenta of the incoming protons as $P_{1,2}^\mu = (\sqrt{S}/2)(1, 0, 0, \pm 1)$ and those of the Reggeized partons as $q_i^\mu = x_i P_i^\mu + q_{iT}^\mu$ ($i = 1, 2$), where x_i are longitudinal momentum fractions and $q_{iT}^\mu = (0, \mathbf{q}_{iT}, 0)$, with \mathbf{q}_{iT} being transverse two-momenta, and we define $t_i = -q_{iT}^2 = \mathbf{q}_{iT}^2$. The final partons have four-momenta $k_{1,2}$ and they are on-shell and massless $k_1^2 = k_2^2 = 0$.

The effective gauge invariant amplitudes for the above mentioned subprocesses (1)-(8) can be obtained using the effective Feynman rules from Refs. [7, 8, 17]. As usual, we introduce the light-cone vectors $n^+ = 2P_2/\sqrt{S}$ and $n^- = 2P_1/\sqrt{S}$, and define $k^\pm = k \cdot n^\pm$ for any four-vector k^μ . Then we determine effective vertices:

$$\Gamma_\mu^{(+-)}(q_1, q_2) = 2 \left[\left(q_1^+ + \frac{q_1^2}{q_2^-} \right) n_\mu^- - \left(q_2^- + \frac{q_2^2}{q_1^+} \right) n_\mu^+ + (q_2 - q_1)_\mu \right], \quad (1)$$

$$\gamma_\mu^\pm(q, p) = \gamma_\mu + \hat{q} \frac{n_\mu^\pm}{p^\pm}, \quad (2)$$

$$\gamma_\mu^{(+-)}(q_1, q_2) = \gamma_\mu - \hat{q}_1 \frac{n_\mu^-}{q_2^-} - \hat{q}_2 \frac{n_\mu^+}{q_1^+}, \quad (3)$$

$$\begin{aligned} \Gamma^{\mu\nu+}(q_1, q_2) &= 2q_1^+ g^{\mu\nu} - (n^+)^\mu (q_1 - q_2)^\nu - (n^+)^\nu (q_1 + 2q_2)^\mu + \frac{t_2}{q_1^+} (n^+)^\mu (n^+)^\nu, \\ \Gamma^{\mu\nu-}(q_1, q_2) &= 2q_2^- g^{\mu\nu} + (n^-)^\mu (q_1 - q_2)^\nu - (n^-)^\nu (q_2 + 2q_1)^\mu + \frac{t_1}{q_2^-} (n^-)^\mu (n^-)^\nu, \end{aligned} \quad (4)$$

and the triple-gluon vertex

$$\gamma_{\mu\nu\sigma}(q, p) = (q - p)_\sigma g_{\mu\nu} - (p + 2q)_\mu g_{\nu\sigma} + (2p + q)_\nu g_{\mu\sigma}. \quad (5)$$

Here we present the two effective amplitudes of the all them for relevant subprocesses, while

the full set of them can be found in the work [14]

$$\begin{aligned}
C_{RR,ab}^{gg, cd, \mu\nu}(q_1, q_2, k_1, k_2) &= g_s^2 \frac{q_1^+ q_2^-}{4\sqrt{t_1 t_2}} \left(T_1 s^{-1} \Gamma^{(+ -)\sigma}(q_1, q_2) \gamma_{\mu\nu\sigma}(-k_1, -k_2) + \right. \\
&+ T_3 t^{-1} \Gamma^{\sigma\mu-}(q_1, k_1 - q_1) \Gamma^{\sigma\nu+}(k_2 - q_2, q_2) - \\
&- T_2 u^{-1} \Gamma^{\sigma\nu-}(q_1, k_2 - q_1) \Gamma^{\sigma\mu+}(k_1 - q_2, q_2) - \\
&- T_1 (n_\mu^- n_\nu^+ - n_\nu^- n_\mu^+) - T_2 (2g_{\mu\nu} - n_\mu^- n_\nu^+) - T_3 (-2g_{\mu\nu} + n_\nu^- n_\mu^+) + \\
&\left. + \Delta^{\mu\nu+}(q_1, q_2, k_1, k_2) + \Delta^{\mu\nu-}(q_1, q_2, k_1, k_2) \right), \quad (6)
\end{aligned}$$

where

$$\begin{aligned}
T_1 &= f_{cdr} f_{abr}, \quad T_2 = f_{dar} f_{cbr}, \quad T_3 = f_{acr} f_{dbr}, \quad T_1 + T_2 + T_3 = 0, \\
\Delta^{\mu\nu+}(q_1, q_2, k_1, k_2) &= 2t_2 n_\mu^+ n_\nu^+ \left(\frac{T_3}{k_2^+ q_1^+} - \frac{T_2}{k_1^+ q_1^+} \right), \\
\Delta^{\mu\nu-}(q_1, q_2, k_1, k_2) &= 2t_1 n_\mu^- n_\nu^- \left(\frac{T_3}{k_1^- q_2^-} - \frac{T_2}{k_2^- q_2^-} \right),
\end{aligned}$$

f^{abc} are structure constants of color gauge group SU(3), $g_s^2 = 4\pi\alpha_s$, and α_s is a strong-coupling constant.

$$\begin{aligned}
\mathcal{M}_{RR, ab}^{q\bar{q}} &= g_s^2 \frac{q_1^+ q_2^-}{4\sqrt{t_1 t_2}} \epsilon_\mu(k_1) \epsilon_\nu(k_2) \bar{U}(k_1) \left(-s^{-1} [T^a, T^b] \gamma^\sigma \Gamma_\sigma^{(+ -)}(q_1, q_2) + \right. \\
&\left. + t^{-1} T^a T^b \gamma^- (\hat{k}_1 - \hat{q}_1) \gamma^+ + u^{-1} T^b T^a \gamma^+ (\hat{k}_1 - \hat{q}_2) \gamma^- \right) V(k_2), \quad (7)
\end{aligned}$$

$$\begin{aligned}
\mathcal{M}_{QR, a}^{qg, b, \mu} &= \frac{g_s^2 q_2^-}{4\sqrt{t_2}} \epsilon_\mu(k_2) \bar{U}(k_1) \left[\gamma_\sigma^{(-)}(q_1, k_1 - q_1) t^{-1} (\gamma_{\mu\nu\sigma}(k_2, -q_2) n_\nu^+ + t_2 \frac{n_\mu^+ n_\sigma^+}{k_2^+}) \times \right. \\
&\times [T^a, T^b] - \gamma^+(\hat{q}_1 - \hat{k}_2)^{-1} \gamma_\mu^{(-)}(q_1, -k_2) T^a T^b - \\
&\left. - \gamma_\mu(\hat{q}_1 + \hat{q}_2)^{-1} \gamma_\sigma^{(-)}(q_1, q_2) n_\sigma^+ T^b T^a + \frac{2\hat{q}_1 n_\mu^-}{k_1^-} \left(\frac{T^a T^b}{k_2^-} - \frac{T^b T^a}{q_2^-} \right) \right] U(x_1 P_1), \quad (8)
\end{aligned}$$

To calculate dijet production cross section we have found squared amplitudes $|\overline{\mathcal{M}}|^2$ of above mentioned subprocesses (1)-(8), where the bar indicates average (summation) over initial-state (final-state) spins and colors. In general case, the squared amplitudes can be written as functions of the Mandelstam variables $s = (q_1 + q_2)^2$, $t = (q_1 - k_1)^2$, $u = (q_1 - k_2)^2$, and invariant Sudakov variables $a_1 = 2k_1 \cdot P_2/S$, $a_2 = 2k_2 \cdot P_2/S$, $b_1 = 2k_1 \cdot P_1/S$, $b_2 = 2k_2 \cdot P_1/S$, in the form

$$|\overline{\mathcal{M}}|^2 = \pi^2 \alpha_s^2 A \sum_{n=0}^4 W_n S^n, \quad (9)$$

where A and W_n are process-dependent functions of variables $s, t, u, a_1, a_2, b_1, b_2, t_1, t_2, S$. The exact analytical formulas for A and W_n are presented in the work [14]. Our definition of the Reggeized amplitudes satisfy evident normalization to the QCD-amplitudes of the collinear parton model:

$$\lim_{t_1, t_2 \rightarrow 0} \int \frac{d\varphi_1}{2\pi} \int \frac{d\varphi_2}{2\pi} |\overline{\mathcal{M}}(t_1, t_2, \varphi_1, \varphi_2)|^2 = |\overline{\mathcal{M}}_{PM}|^2. \quad (10)$$

that has been checked for all obtained squared matrix elements.

According to the high-energy factorization formalism, the proton-proton production cross section for dijets is obtained by the convolution of squared matrix element $|\overline{\mathcal{M}}|$ with the unintegrated Reggeized PDFs $\Phi_{g(q)}^p(x_{1,2}, t_{1,2}, \mu^2)$ at the factorization scale μ [20]. Here we present an analytic formula for the case of the subprocess (1), and the other can be written in the same manner:

$$\frac{d\sigma(pp \rightarrow ggX)}{dk_{1T}dy_1dk_{2T}dy_2d\Delta\varphi} = \frac{k_{1T}k_{2T}}{16\pi^3} \int dt_1 \int d\phi_1 \Phi_g^p(x_1, t_1, \mu^2) \Phi_g^p(x_2, t_2, \mu^2) \frac{|\overline{\mathcal{M}}(RR \rightarrow gg)|^2}{(x_1x_2S)^2}, \quad (11)$$

where $k_{1,2T}$ and $y_{1,2}$ are final gluon transverse momenta and rapidities, respectively, and $\Delta\varphi$ is an azimuthal angle enclosed between the vectors \vec{k}_{1T} and \vec{k}_{2T} ,

$$x_1 = (k_1^0 + k_2^0 + k_1^z + k_2^z)/\sqrt{S}, \quad x_2 = (k_1^0 + k_2^0 - k_1^z - k_2^z)/\sqrt{S},$$

$$k_{1,2}^0 = k_{1,2T} \cosh(y_{1,2}), \quad k_{1,2}^z = k_{1,2T} \sinh(y_{1,2}).$$

Throughout our analysis the renormalization and factorization scales are identified and chosen to be $\mu = \xi k_{1T}$, where k_{1T} is the transverse momentum of the leading jet ($k_{1T} > k_{2T}$) and ξ is varied between 1/2 and 2 about its default value 1 to estimate the theoretical uncertainty due to the freedom in the choice of scales. The resulting errors are indicated as shaded bands in the figures.

The unintegrated PDFs $\Phi_g^p(x, t, \mu^2)$ are related to their collinear counterparts $f_g^p(x, \mu^2)$ by the normalization condition

$$x f_g^p(x, \mu^2) = \int^{\mu^2} dt \Phi_g^p(x, t, \mu^2), \quad (12)$$

which furnishes a correct transition from formulas in parton Reggeization approach to those in the collinear parton model. In our numerical analysis, we adopt the prescription proposed by Kimber, Martin, and Ryskin (KMR) [18] to obtain the unintegrated gluon and quark PDFs of the proton from the conventional integrated ones. As input for these procedures, we use the LO set of the Martin-Roberts-Stirling-Thorne (MRST) [19] proton PDFs as our default.

3 Results

Recently, CMS [2] and ATLAS [3] Collaborations have measured azimuthal decorrelations between the two central jets with the highest transverse momenta (leading jets) and rapidity $p_T > 30$ GeV, $|y| < 1.1$, and $p_T > 100$ GeV, $|y| < 0.8$, correspondingly, in proton-proton collisions at $\sqrt{S} = 7$ TeV. The measurements are presented for the region of $\pi/2 < \Delta\varphi < \pi$ as normalized distributions $F(\Delta\varphi) = \frac{1}{\sigma} \times \left(\frac{d\sigma}{d\Delta\varphi} \right)$, where $\sigma = \int_{\pi/2}^{\pi} \left(\frac{d\sigma}{d\Delta\varphi} \right) d\Delta\varphi$. Additionally, the ATLAS Collaboration presented the $\Delta\varphi$ distribution of events with ≥ 2 , ≥ 3 , ≥ 4 , and ≥ 5 jets with $p_T > 100$ GeV and $|y| < 0.8$ for the leading jets and $|y| < 2.8$ for all other jets.

The theoretical expectations based on the collinear parton model for $\Delta\varphi$ distributions include pQCD calculation in NLO (α_S^4) for the three-parton final states and LO (α_S^4) for the four-parton final states [21]. As it has been demonstrated in Refs. [2, 3], these calculations describe data in the region of $2\pi/3 < \Delta\varphi < \pi$ and overestimate data at $\Delta\varphi < 2\pi/3$. The agreement of parton model calculations with data can be achieved using the Monte Carlo event generators (MC), such as: PYTHIA [22], HERWIG++ and MADGRAPH [23], which include NLO pQCD matrix elements, different collinear PDFs, effects of hadronization and the initial-state parton shower radiation (ISR). The latter is very important to simulate events at $\Delta\varphi < 2\pi/3$ but introducing a new theoretically unknown parameter k_{ISR} which can be fixed phenomenologically only.

To obtain a distribution $F(\Delta\phi)$ in the frameworks of the PRA, we perform an integration of the differential cross section (11) over the final-state parton transverse momenta k_{1T} and k_{2T} , as well as over the rapidities y_1 and y_2 in the intervals defined by the experiment. We take into account contributions of all subprocesses (1)-(8), where quark flavors are taken $q = u, d, s$ for initial-state and final-state quarks. The upper limit for the Reggeized-gluon transverse momenta squared t_1 and t_2 is taken as $t_1, t_2 < k_{2T}^2$, where k_{2T} is a smaller transverse momentum of a jet from the pair of two leading jets. This condition arises from the experimental constraint that it is impossible to separate final-state partons produced in the hard parton scattering phase from the ones generated during QCD-evolution of PDFs. The BFKL evolution suggests a strong ordering in rapidity but transverse momenta of partons in the QCD-ladder keep similar values. It means, that the transverse momenta of partons generated in the initial-state evolution, described via the unintegrated PDF must be smaller than transverse momenta of both measured leading jets.

The predictions of the LO PRA for the CMS measurements [2] of $F(\Delta\phi)$ distributions for the two most energetic jets are shown in Fig. 1, which demonstrates a nice agreement in the region of $\Delta\phi \geq 3\pi/4$. As $\Delta\phi$ decreases from $3\pi/4$ to $\pi/2$, the theoretical expectations tend to underestimate data more and more, up to a factor 5 at the $80 < p_T^{max} < 110$ GeV and a factor 2 at the $200 < p_T^{max} < 300$ GeV. This difference follows from our theoretical approximation: we take into account only two-jet production subprocesses in the QMRK, like the $RR \rightarrow gg$. However, at $\Delta\phi \simeq \pi/2$, the contribution of three-jet production subprocess should be important. One can find, the difference becomes smaller with growing of p_T^{max} , because the situation when transverse momentum of leading jet is compensated by the one energetic jet in opposite direction is more probable than the such compensation by two or more jets.

Our observations are confirmed in Fig. 2, where the disagreements between our calculations and ATLAS data [3] are smaller than in the case of CMS data, because the low- p_T cut made by ATLAS Collaboration, $p_T > 110$ GeV, exceeds the CMS one, $p_T > 30$ GeV.

Certainly, the precise comparison of theoretical predictions in the LO PRA should be performed when we separate only the two-jet production in the central rapidity region. The ATLAS Collaboration presents the $\Delta\phi$ -distributions for different number of final-state jets (see Fig. 1 in Ref. [3]) for the kinematic domain of $p_T^{max} > 100$ GeV and $|y| < 0.8$. We can extract $F(\Delta\phi)$ for only two-jet production from these data as a difference between number of events: $n(2) = n(\geq 2) - n(\geq 3)$ or $\sigma(2)F(\Delta\phi, 2) = \sigma(\geq 2)F(\Delta\phi, \geq 2) - \sigma(\geq 3)F(\Delta\phi, \geq 3)$. The original ATLAS data for $F(\Delta\phi, \geq 2)$ and extracted data for $F(\Delta\phi, 2)$ are shown together with our predictions in Fig. 3, and a nice agreement of the two latter is obtained.

Summarizing results of a present analysis for dijet production at the LHC and our previous study of $b\bar{b}$ -pair production at the Tevatron and LHC [12, 13], we find a strong difference of theoretical interpretation of azimuthal decorrelation between leading and subleading jets, in the collinear parton model and in the parton Reggeization approach. In the first case, an azimuthal decorrelation at different values of $\Delta\phi$ is provided by hard $2 \rightarrow 3$ ($3\pi/4 < \Delta\phi < \pi$), $2 \rightarrow 4$ ($\pi/2 < \Delta\phi < 3\pi/4$) partonic subprocesses, correspondingly. The explanation of data in the region of $\Delta\phi < \pi/2$ in the framework of collinear parton model becomes possible only because of initial-state radiation and hadronization effects, and an agreement of theory expectations and data is achieved using MC generators only.

Oppositely, in the parton Reggeization approach, the azimuthal decorrelation is explained by the coherent parton emission during the QCD-evolution, which is described by the transverse-momentum dependent PDFs of Reggeized partons. Already in the LO approximation, at the level of $2 \rightarrow 2$ subprocesses with Reggeized partons, we can account the main part of decorrelation effect in dijet production, and we obtain a full description of data in $b\bar{b}$ -pair production.

4 Conclusions

This good description of dijet azimuthal decorrelations is achieved in the LO parton Reggeization approach, without any ad-hoc adjustments of input parameters. By contrast, in the collinear parton model, such a degree of agreement calls for NLO and NNLO corrections and complementary initial-state radiation effects and ad-hoc nonperturbative transverse momenta of partons. In conclusion, the parton Reggeization approach has once again proven to be a powerful tool for the theoretical description of QCD processes induced by Reggeized partons in the high-energy limit. As it was shown by the recent studies [24], the one-loop calculations in this formalism lead the results for the NLO effective vertices, consistent with the earlier calculations based on unitarity relations [25]. These results open a possibility to extend the calculations of hard processes in the parton Reggeization approach to the complete-NLO level.

Acknowledgements

We are grateful to B. A. Kniehl, E. A. Kuraev, L. N. Lipatov and N. N. Nikolaev for useful discussions. The work of A. V. Shipilova and M.A. Nefedov was partly supported by the Grant of President of Russian Federation No. MK-4150.2014.2. The work of M.A. Nefedov and V.A. Saleev was supported in part by the Russian Foundation for Basic Research through the Grant No. 14-02-00021.

References

- [1] B.L. Ioffe, V.S. Fadin and L.N. Lipatov, Quantum chromodynamics. Perturbative and nonperturbative aspects. Cambridge University Press, 2010, Cambridge, UK; D. Green, High p_T physics at hadron colliders. Cambridge University Press, 2005, Cambridge, UK.
- [2] CMS Collaboration, V. Khachatryan et al., Phys. Rev. Lett. **106**, 122003 (2011).
- [3] ATLAS Collaboration, G. Aad et al., Phys. Rev. Lett. **106**, 172002 (2011).
- [4] B. A. Kniehl, V. A. Saleev, A. V. Shipilova, E. V. Yatsenko, Phys. Rev. **D84**, 074017 (2011).
- [5] V. S. Fadin and L. N. Lipatov, Nucl. Phys. **B406**, 259 (1993); **B477**, 767 (1996).
- [6] V. S. Fadin and V. E. Sherman, JETP Lett. **23**, 599 (1976); JETP **45**, 861 (1977).
- [7] L. N. Lipatov, Nucl. Phys. **B452**, 369 (1995).
- [8] L. N. Lipatov and M. I. Vyazovsky, Nucl. Phys. **B597**, 399 (2001).
- [9] V. A. Saleev, Phys. Rev. D **78**, 034033 (2008).
- [10] V. A. Saleev, Phys. Rev. D **78**, 114031 (2008).
- [11] M.A. Nefedov, N.N. Nikolaev, and V.A. Saleev, Phys. Rev. D **87**, 014022 (2013).
- [12] B. A. Kniehl, A. V. Shipilova, and V. A. Saleev, Phys. Rev. D **81**, 094010 (2010).
- [13] V.A. Saleev, A.V. Shipilova, Phys. Rev. **D86**, 034032 (2012).
- [14] M. A. Nefedov, V. A. Saleev, A. V. Shipilova Phys. Rev. D. **87**, 094030 (2013).

- [15] L. N. Lipatov, Sov. J. Nucl. Phys. **23**, 338 (1976) [Yad. Fiz. **23**, 642 (1976)]; E. A. Kuraev, L. N. Lipatov, and V. S. Fadin, Sov. Phys. JETP **44**, 443 (1976) [Zh. Eksp. Teor. Fiz. **71**, 840 (1976)]; Sov. Phys. JETP **45**, 199 (1977) [Zh. Eksp. Teor. Fiz. **72**, 377 (1977)]; I. I. Balitsky and L. N. Lipatov, Sov. J. Nucl. Phys. **28**, 822 (1978) [Yad. Fiz. **28**, 1597 (1978)]; Sov. Phys. JETP **63**, 904 (1986) [Zh. Eksp. Teor. Fiz. **90**, 1536 (1986)].
- [16] V. N. Gribov and L. N. Lipatov, Sov. J. Nucl. Phys. **15**, 438 (1972) [Yad. Fiz. **15**, 781 (1972)]; Yu. L. Dokshitzer, Sov. Phys. JETP **46**, 641 (1977) [Zh. Eksp. Teor. Fiz. **73**, 1216 (1977)]; G. Altarelli and G. Parisi, Nucl. Phys. **B126**, 298 (1977).
- [17] E. N. Antonov, L. N. Lipatov, E. A. Kuraev, and I. O. Cherednikov, Nucl. Phys. **B721**, 111 (2005).
- [18] M. A. Kimber, A. D. Martin, and M. G. Ryskin, Eur. Phys. J. C **12**, 655 (2000); Phys. Rev. D **63**, 114027 (2001); G. Watt, A. D. Martin, and M. G. Ryskin, Eur. Phys. J. C **31**, 73 (2003).
- [19] A. D. Martin, W. J. Stirling, R. S. Thorne, Phys. Lett. **B636** 259 (2006).
- [20] V.A. Saleev, Phys. Rev. D **80**, 114016 (2009).
- [21] Z. Nagy, Phys. Rev. Lett. **88**, 122003 (2002).
- [22] T. Sjostrand, S. Mrenna, and P. Skands, Comput. Phys. Commun. **178**, 852 (2008).
- [23] J. Alwall et al., J. High Energy Phys. **09**, 028 (2007)
- [24] M. Hentschinski, A. Sabio Vera, Phys. Rev. **D85**, 056006 (2012), G. Chachamis, M. Hentschinski, J. D. Madrigal, A. Sabio Vera, [arXiv: 1212.4992 [hep-ph]] (2012).
- [25] V. Fadin, R. Fiore, A. Quartarolo, Phys. Rev. **D50**, 2265 (1994), Phys. Rev. **D50**, 5893 (1994), V. S. Fadin, R. Fiore, M. I. Kotsky, A. Papa, Phys. Rev. **D61**, 094005 (2000) V. S. Fadin, R. Fiore, A. Papa, Phys. Rev. **D63**, 034001 (2000).

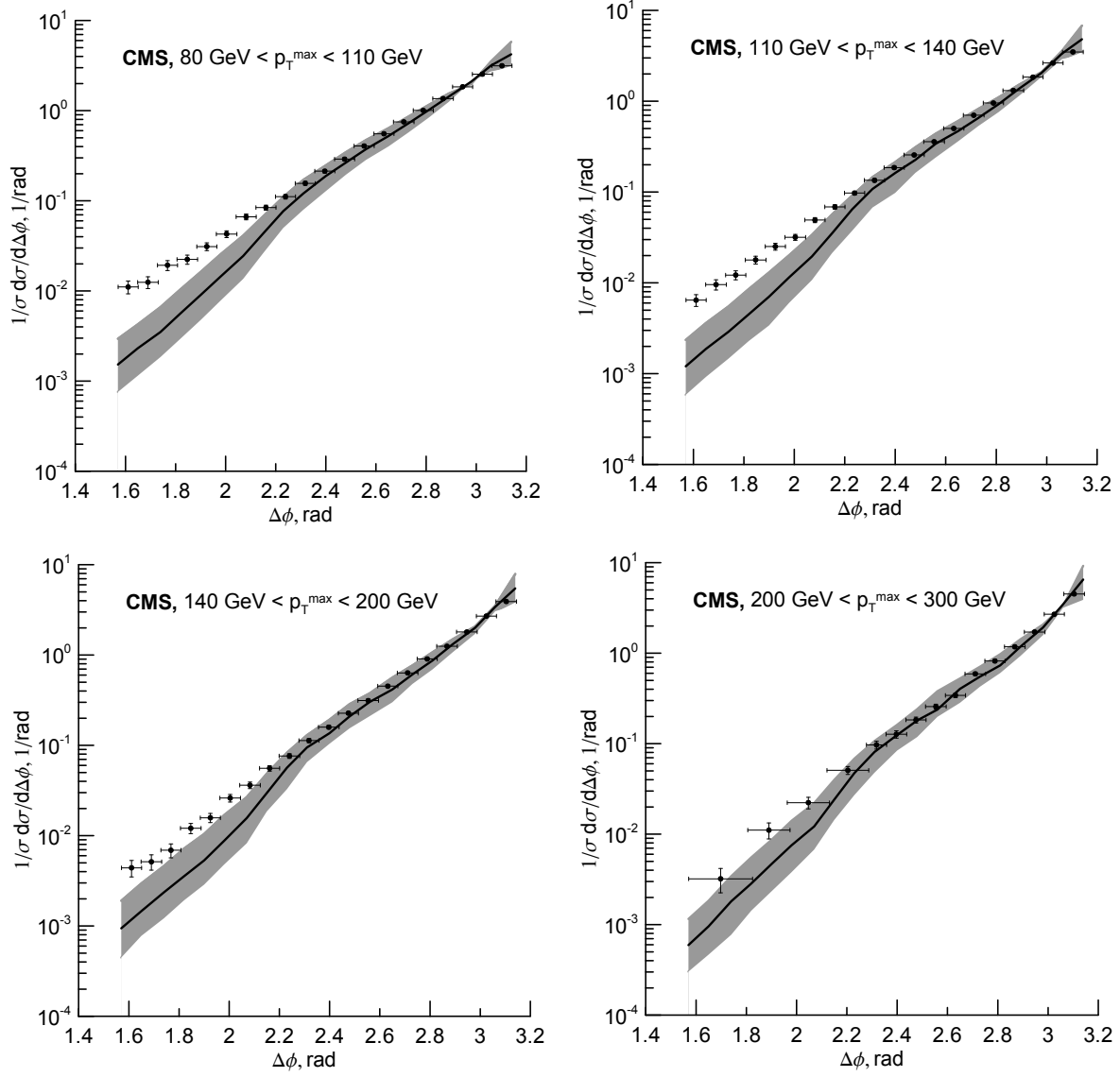


Figure 1: Normalized $F(\Delta\phi)$ distributions in several p_T^{max} regions at the $\sqrt{S} = 7$ TeV, $|y| < 1.1$ and $p_T > 30$ GeV. The data are from the CMS Collaboration [2]. The curve corresponds to LO parton Reggeization approach.

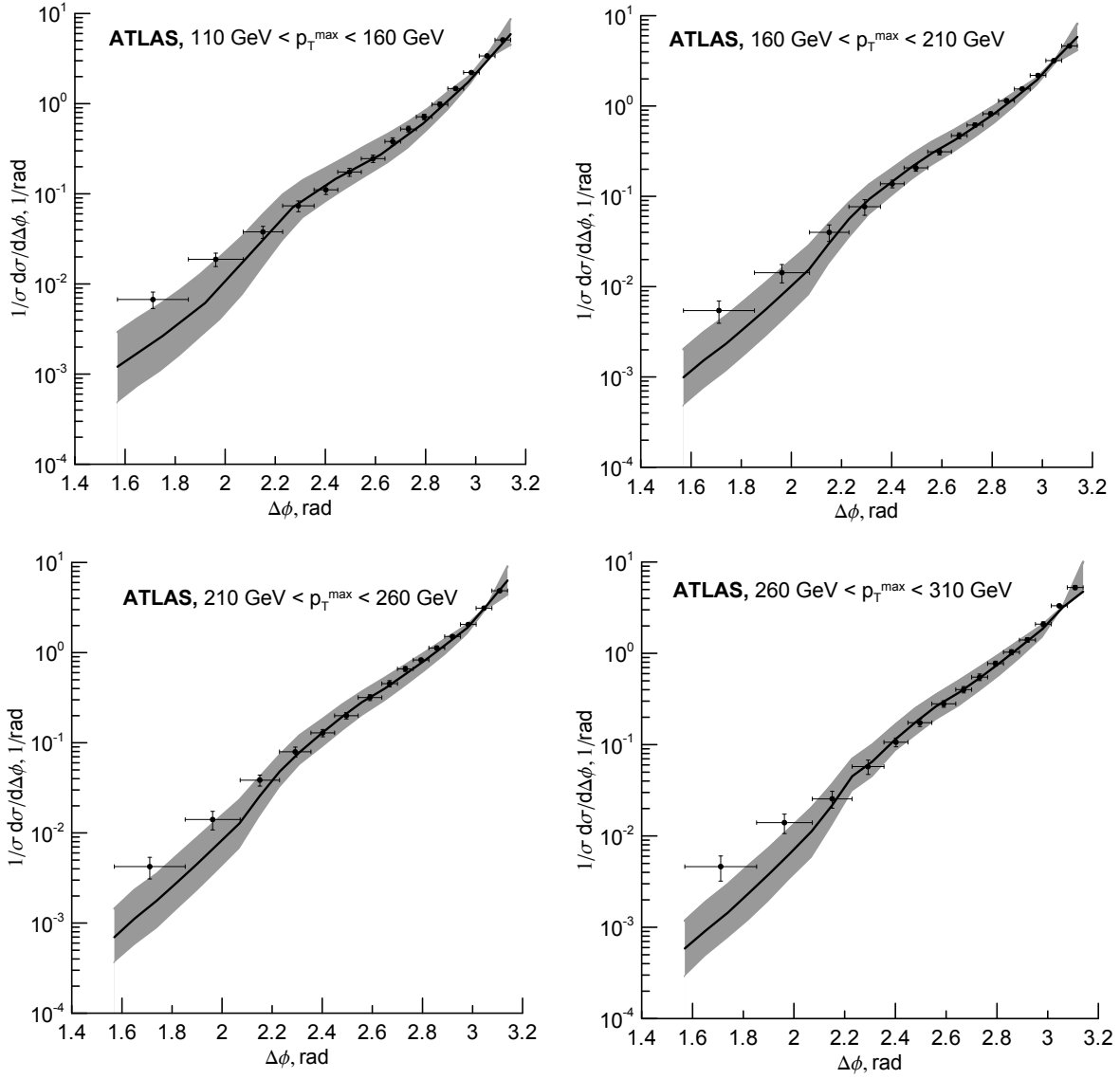


Figure 2: Normalized $F(\Delta\phi)$ distributions in several p_T^{max} regions at the $\sqrt{S} = 7$ TeV, $|y| < 0.8$ and $p_T > 100$ GeV. The data are from the ATLAS Collaboration [3]. The curve corresponds to LO parton Reggeization approach.

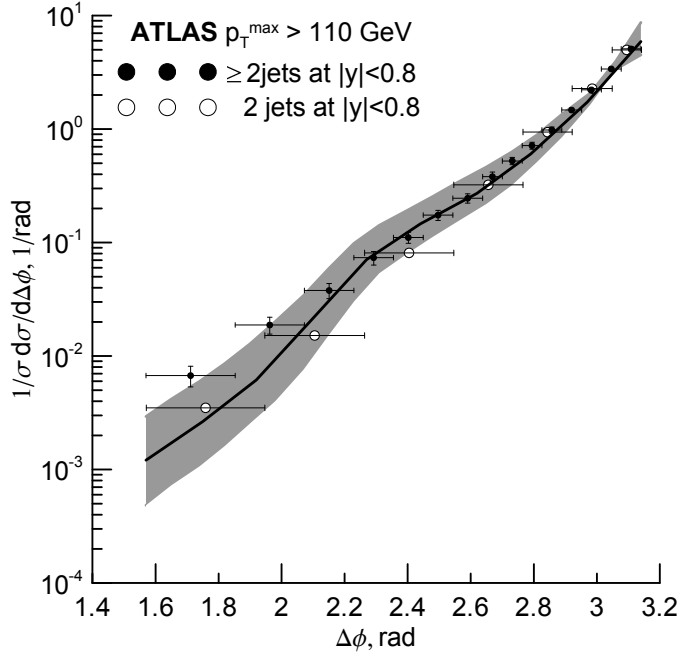


Figure 3: Normalized $F(\Delta\phi)$ distribution for 2 (open circles) and ≥ 2 (black circles) jets with $p_T > 100$ GeV, $|y| < 0.8$, $p_T^{max} > 110$ GeV and $\sqrt{S} = 7$ TeV. The data are from the ATLAS Collaboration [3]. The curve corresponds to LO parton Reggeization approach.